Engineering Structures 57 (2013) 594–608

Contents lists available at SciVerse ScienceDirect

Engineering Structures

journal homepage: www.elsevier.com/locate/engstruct

Pseudodynamic tests on a full-scale 3-storey precast concrete building: Global response

Paolo Negro [a], Dionysios A. Bournas [b,*], Francisco J. Molina [a]

[a] European Laboratory for Structural Assessment, Institute for the Protection and Security of the Citizen, Joint Research Centre, European Commission, T.P. 480, I-21020 Ispra (VA), Italy
[b] Dep. of Civil Engineering, University of Nottingham, NG7 2RD Nottingham, UK

ARTICLE INFO

Article history:
Available online 23 July 2013

Keywords:
Precast concrete structures
Pseudodynamic tests
Safecast project
Beam–column joints
Diaphragm
Dry connections
Mechanical connections
Shear walls

ABSTRACT

In the framework of the SAFECAST Project, a full-scale three-storey precast building was subjected to a series of pseudodynamic (PsD) tests in the European Laboratory for Structural Assessment (ELSA). The mock-up was constructed in such a way that four different structural configurations could be investigated experimentally. Therefore, the behaviour of various parameters like the types of mechanical connections (traditional as well as innovative) and the presence or absence of shear walls along with the framed structure were investigated. The first PsD tests were conducted on a dual frame-wall precast system, where two precast shear wall units were connected to the mock up. The first test structure sustained the maximum earthquake for which it had been designed with small horizontal deformations. In the second layout, the shear walls were disconnected from the structure, to test the building in its most typical configuration, namely with hinged beam–column connections by means of dowel bars (shear connectors). This configuration was quite flexible and suffered large deformations under the design level earthquake. An innovative connection system, embedded in the precast elements, was then activated to create emulative beam–column connections in the last two structural configurations. In particular, in the third layout the connectors were restrained only at the top floor, whereas in the fourth layout the connection system was activated in all beam–column joints. The PsD test results showed that, when activated at all the floors, the proposed connection system is quite effective as a means of implementing dry precast (quasi) emulative moment-resisting frames.

1. Introduction and background

A collaborative three-year research project called SAFECAST was undertaken by European national associations of precast concrete producers, along with universities and research centres, to study the behaviour of precast concrete structures under earthquake loading. The main objective of the project was to fill the gap in the knowledge of seismic behaviour of precast concrete structures, with emphasis on the connections between precast members. A major part of the experimental phase of this programme consisted of the pseudodynamic tests on a full-scale 3-storey precast concrete building, carried out at the European Laboratory for Structural Assessment (ELSA), Joint Research Centre (JRC) of the European Commission in Ispra.

Precast concrete construction represents a viable alternative to construction methods utilizing cast-in-place concrete. Advantages related to the use of precast techniques include higher quality control that can be obtained in the precast plants, speed of erection, and freedom in the architectural shape of the members. Despite these well-recognized advantages, the use and development of precast concrete structures in seismic areas have been typically limited by the lack of confidence and knowledge about their seismic performance.

ASSOBETON (the Italian association of precast producers) and the ELSA Laboratory of the Joint Research Centre have a long tradition of scientific collaboration on the subject of the seismic behaviour of precast structures. The two institutions have been involved in the study of the seismic behaviour of precast structures elements since 1994 [1]. After the identification of the seismic behaviour of single elements, a research programme aimed at demonstrating the equivalence between the behaviour factor of precast and cast-in situ single-storey industrial buildings was activated. This research project, named "Seismic behaviour of precast R/C industrial buildings", partially financed within the European "Ecoleader" research programme was performed at the ELSA Laboratory. The results of the tests demonstrated the excellent capacity of precast buildings to withstand earthquakes without suffering important damage [2]. The data obtained within the two mentioned research projects provided the starting point for the PRECAST EC8 project [3]. This project was successfully carried out

* Corresponding author. Tel.: +44 0115 951 4096.
E-mail addresses: paolo.negro@jrc.ec.europa.eu (P. Negro), dionysios.bournas@nottingham.ac.uk (D.A. Bournas), francisco.molina@jrc.ec.europa.eu (F.J. Molina).

0141-0296/$ - see front matter © 2013 Elsevier Ltd. All rights reserved.
http://dx.doi.org/10.1016/j.engstruct.2013.05.047

and concluded in early 2007, after 4 years of activity. As a result of the project, a calibration of the global behaviour factor (q factor) for precast frame structures was carried out with a combined experimental and numerical approach. The research pointed out the very good behaviour of precast structures under earthquake conditions and their substantial equality to traditional cast-in situ ones as for the safety under earthquake excitation, even without monolithic joints.

The only, but crucial missing link in the modelling of such precast buildings, was the adequate knowledge about the behaviour of connections. The empirical evidence from the past earthquakes is sparse, incomplete, non-quantified and first of all controversial. Some reports show excellent behaviour of precast systems and connections [4–6]. On the other hand, the same documents report some catastrophic collapses. This is not surprising, since seismic response clearly depends on the specific structural system, type of connections and quality of the design and construction. Some collapses were also reported during the 1977 Vrancea earthquake [7], the 1979 Montenegro earthquake [8] and the Northridge earthquake [9]. Failures of welded and poorly constructed connections were also the main cause of extensive collapses in Armenia [10] and during the 1976 Tangshan earthquake in China. These bad experiences have generated mistrust to precast systems in general. In some countries this practically preclude the use of precast structures and in many codes all precast systems were penalized with high seismic forces related to the reduced competitiveness in the market.

The problem of investigating the seismic behaviour of connection among precast concrete elements is addressed within the SAFECAST project. The major part of the experimental phase of this programme comprises the pseudodynamic tests on full-scale 3-storey precast concrete prototypes. The paper presents the global test results related to the overall pseudodynamic response of the prototypes.

2. Design of the prototype according to Eurocode 8

The prototype was designed with the aim of providing experimental validation about the seismic behaviour of multi-storey precast concrete buildings, through large-scale reference testing. The aim of this campaign was to provide proper experimental evidences about the seismic behaviour of precast multi-storey buildings with both hinged and moment-resisting beam-to-column connections. The building was representative of a large-scale three-storey building with a 7 m by 7 m structural grid with and without structural walls. Its portion that was (initially) selected to be tested had 2 by 3 spans/bays (14 by 21 m). However, the dynamic non-linear analyses conducted [11,12] revealed the possible effects of the higher vibration modes on this type of relatively-"flexible"-structure. In particular, the storey forces obtained from these analyses exceeded the force capacity of the available actuators in some of the floors. Thus, the prototype that was finally decided to be constructed and tested comprised a 2 by 2 spans/bays structure as presented in next section.

3. Test structures

3.1. The mock-up

The specimen structure was a three-storey full-scale precast residential building, with two 7 m bays in each horizontal direction as shown in Fig. 1a. The structure was 15 × 16.25 m in plan and had a height of 10.9 m (9.9 m above the foundation level) with floor-to-floor heights equal to 3.5 m, 3.2 m and 3.2 m for the 1st, 2nd and 3rd level, respectively. Whereas the storey height is typically larger in single-storey industrial or commercial precast buildings, those of the specimen well represent the typical configuration for a residential or office building in Europe.

The floor systems which were of high interest in this research, were carefully selected to gather the largest possible useful information. To accomplish this, three different pretopped floor systems were adopted. As shown in Fig. 1b and c, the 1st floor at 3.5 m was constructed with box-type elements put side by side and welded to each other; similarly the 2nd floor at 6.7 m comprised double-tee elements put side by side welded to each other; and finally the 3rd floor at 9.9 m was realized with the same box slab elements of the 1st floor, but spaced to simulate diaphragms with openings. Detailed description of the three floor systems and their connections is given in the companion paper by Bournas et al. [13].

The precast three-storey columns had a cross-section of 0.5 × 0.5 m (Fig. 2a) which was kept constant along their height and were embedded by 0.75 m into 1-m-deep 1.3 × 1.3 m in plan, pocket foundations (Fig. 2b). All the columns were constructed with wide capitals at the level of each floor, with widths of 0.90 m and 2.25 m in the loading and transverse direction, respectively (Fig. 2c), in order to allow for the mechanical beam-to-column connection, the details of which are presented in a companion paper. The capitals of the columns were designed as cantilevers fixed at the axis of the columns with flexure and shear reinforcement. Fig. 2d illustrates the erection phase of a column with capitals before its positioning into the pocket foundation.

The longitudinal beams connected to the columns' capitals were precast box-type hollow core elements, with a cross-section 0.4 × 2.25 m and a length of 6.38 m. The cross section and dimensions of a typical beam spanning in the direction of loading are illustrated in Fig. 3. Such type of beam has similar weight with respect to its equivalent inverted T or I-shaped beam in terms of stiffness but with clear economical advantages over it associated with the increase in the floor area.

As it can be seen in Fig. 1b, two 4.05-m-long × 9.6-m-tall × 0.25-m-thick (4.05 m × 9.6 m × 250 mm) precast concrete walls were connected to the mock-up in order to compose with the columns a dual frame-wall precast system. Each wall comprised three wall hollow-core precast elements 3.2-m-tall (Fig. 4a) which were joined among themselves by means of vertical reinforcement crossing their gaps at the level of each floor. Concrete was cast only at the two edge cores of the section, where the wall vertical reinforcement was concentrated in "boundary elements". The confinement of the concrete was also limited there (Fig. 4b and c). Thus, the wall's moment resistance was assigned to the "flanges" at the edges of its section and its shear resistance to the "web" in-between them. The nonlinear behaviour of such pre-fabricated walls was expected to differ from the one of normal cast in situ walls, however, this aspect was not considered in the research, since the walls were expected to suffer limited yielding during the test. The longitudinal reinforcement was lap-spliced at the mid-height of the second floor. The walls-to-foundation connection was realized through two pocket foundations in which only the walls' longitudinal reinforcement protruding from the pockets was anchored (Fig. 4d). The connection between the walls and the frame was conceived having in mind the need to easily disconnect the walls at the end of the first round of tests and consisted into over-reinforced blocks of concrete, with steel surfaces, placed at each storey and to be simply cut at the end. This arrangement was neither typical, nor code-compliant; however, in this case the objective was to study the behaviour of the frame as connected to a wall system, rather than studying the behaviour of the wall itself or the connection between the wall and the frame.

All precast elements (columns, walls, beams, slabs) were cast using the same concrete class, namely C45/55, which turned out to havea 28-day strength, measured on 150 × 150 mm cubes,

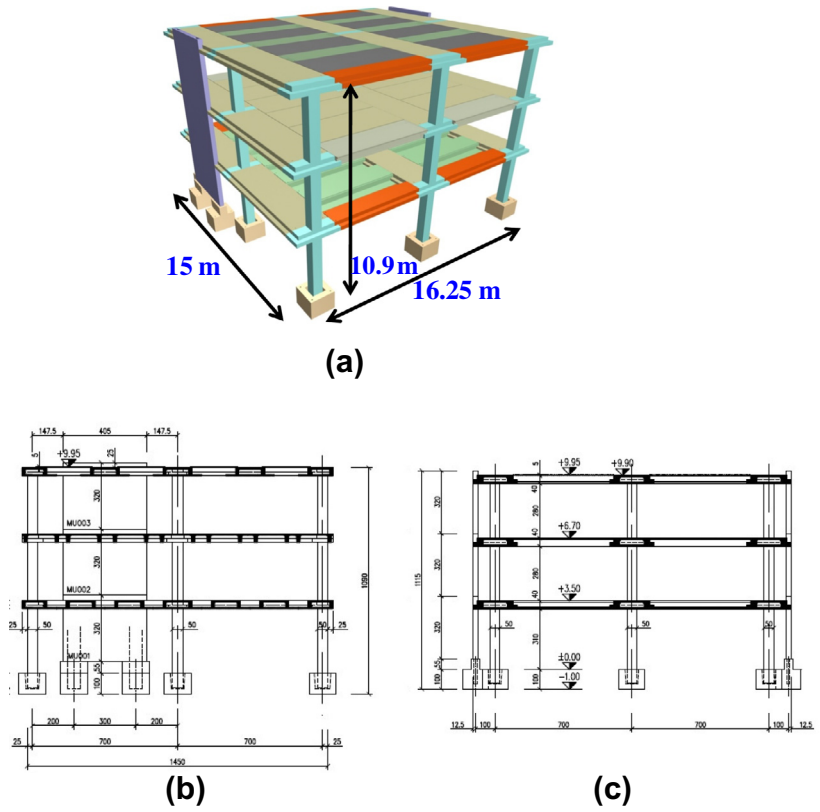

Fig. 1. (a) Three-dimensional representation of the test structure (Dimensions in m). Section view of the test structure: (b) In the loading direction. (c) In the transverse to the loading direction (dimensions in cm).

equal to 64.5 MPa. The corresponding compressive strength of the concrete cast in the boundary elements of the walls was equal to 61 MPa. The steel reinforcement cast into the members had a yield stress of 527 MPa, a tensile strength of 673 MPa, and an ultimate strain equal to 10%. Table 1 summarizes the dimensions and percentages of steel reinforcement of all prefabricated structural bearing elements used for the construction of the mock-up.

It is worth mentioning that the mock-up which weighed approximately 450 t, represents the biggest precast structure ever tested and with a floor area of 244 m^2 (15 × 16.25 m in plan) is possibly also the biggest in plan specimen tested ever under seismic conditions worldwide.

3.2. Description of the structural system-investigated parameters

The mock-up was constructed in such a way that the effectiveness of four different structural precast systems could be investigated experimentally. Therefore, the behaviour of a series of parameters, including several types of mechanical connections (traditional as well as innovative) and the presence or absence of shear walls along with the framed structure, could be assessed.

The first layout (prototype 1) comprised a dual frame-wall precast system, where the two precast shear wall units were connected to the mock-up (Fig. 5a). In this structural configuration, the effectiveness of precast shear walls in terms of increasing the stiffness of a relatively flexible three-storey precast building with hinged beam-to column joints was examined.

In the second layout (prototype 2 – Fig. 5b), the shear walls were disconnected from the structure, to test the building in its most typical configuration, namely with hinged beam–column connections by means of dowel bars (shear connectors). This configuration, which represents the most common connection system in the construction practice in the European countries, had been tested only for industrial typically single-storey precast structures [3]. Thus, the second layout investigated for the first time experimentally the seismic behaviour of a flexible multi (three)-storey precast building with hinged beam-to-column connections, where the columns are expected to work principally as cantilevers.

Afterwards, the possibility of achieving emulative moment resisting frames by means of a new connection system with dry connections was investigated in the third and fourth structural configurations. With the target of providing continuity to the longitudinal reinforcement crossing the joint, an innovative connection system, embedded in the precast elements, was then activated by means of bolts connecting the steel devices in the columns and beams. A special mortar was placed to fill the small gaps between beams and columns. In particular, the first solution examined was expected to combine ease in the implementation and to reduce significantly the flexibility of such structures with hinged beam-to-column joints by restraining just the last floor of multi-storey buildings; and thus, in the third layout (prototype 3 – Fig. 5c) the connectors were restrained only at the third floor. Finally, in the last fourth layout, the connection system was activated in all beam–column joints (prototype 4 – Fig. 5d). A summary of all structural systems and the investigated parameters is presented in Table 2.

4. Experimental programme

4.1. Pseudodynamic testing

The continuous PsD method developed at the ELSA laboratory of the European Commission JRC [14] was used for testing the mock-up. The PsD method couples the properties of the structure as a

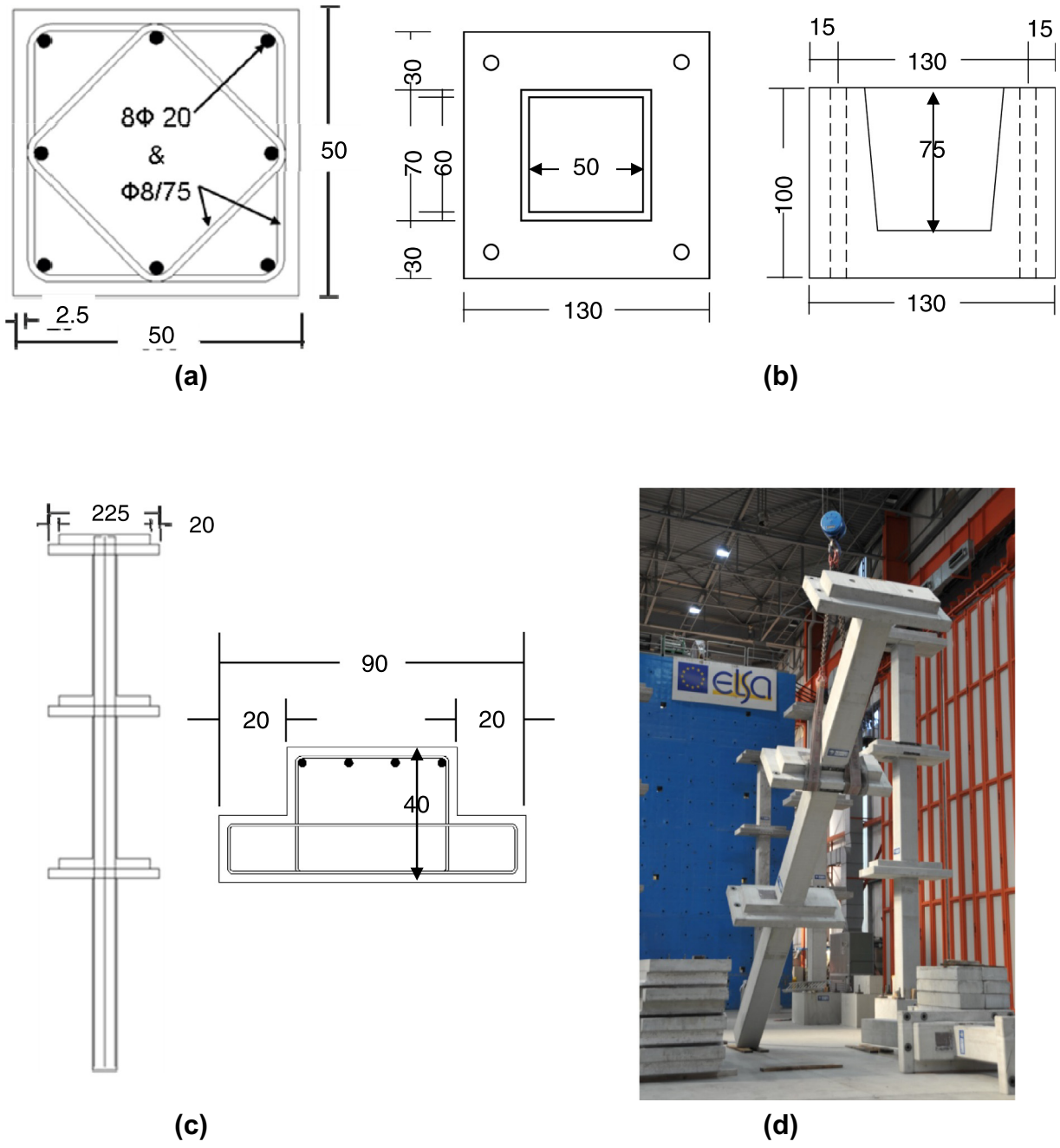

Fig. 2. (a) Cross section of columns. (b) Pocket foundation. (c) A three storey column with its capitals. (d) Erection of a column with capitals (dimensions in cm).

physical quasistatic model tested in the laboratory and a computer model representing inertia. The equation of motion for such an idealized model can be expressed in terms of a second-order ordinary differential equation:

$$Ma(t) + Cv(t) + R(t) = -MIa_g(t) \quad (1)$$

This implies that the structure can be analyzed as if it was supported on a fixed foundation and subjected to an effective force vector $P_{eff}(t) = -MIa_g(t)$, where I is a vector of zeros and ones and $a_g(t)$ is the ground acceleration time history. The mass matrix, M, the viscous damping matrix, C (typically null as explained in [15]), and the excitation force vector, $P_{eff}(t)$, are all numerically specified. The restoring force vector, $R(t)$, which is, in principle, nonlinear with respect to the displacement vector, $d(t)$, is measured experimentally. At each time instant, t, the equation is numerically solved (in this case, through the Explicit Newmark method), from the restoring forces, $R(t)$, measured at time t by the actuator load cells, to obtain the acceleration response, $a(t)$,velocity, $v(t)$ and displacement, $d(t + \Delta t)$, at the next time step. The computed displacements at time instant $t + \Delta t$ are then imposed on the structure *via* actuators which load cells, at the end of the step, provide the (measured) restoring forces, $R(t + \Delta t)$, to be used subsequently for the calculation of the response at the next time step. In the present tests the equation of motion, Eq. (1), was formulated in terms of three degrees of freedom (DOFs), namely one per floor with the floor displacement x parallel to the direction of the excitation at the storey centre of mass. The computed floor displacement was symmetrically imposed at two HEIDENHAIN

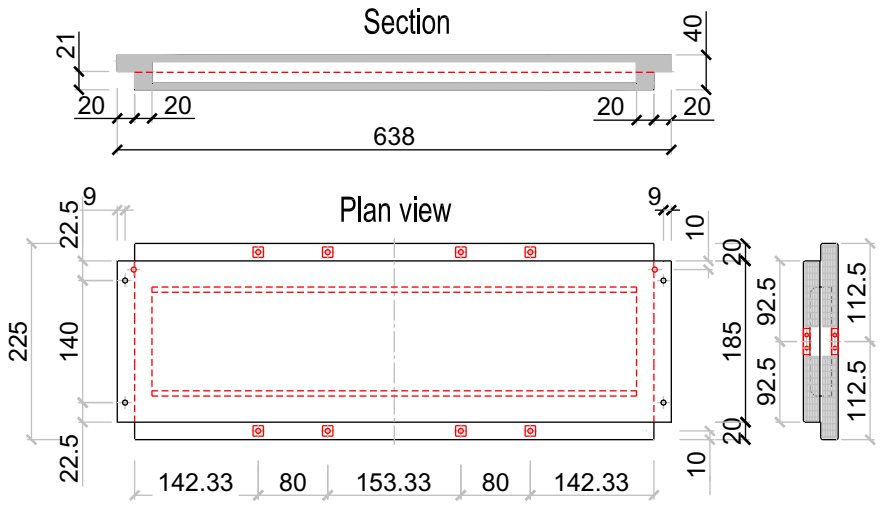

Fig. 3. (a) Cross section and dimensions of the main beams (dimensions in cm).

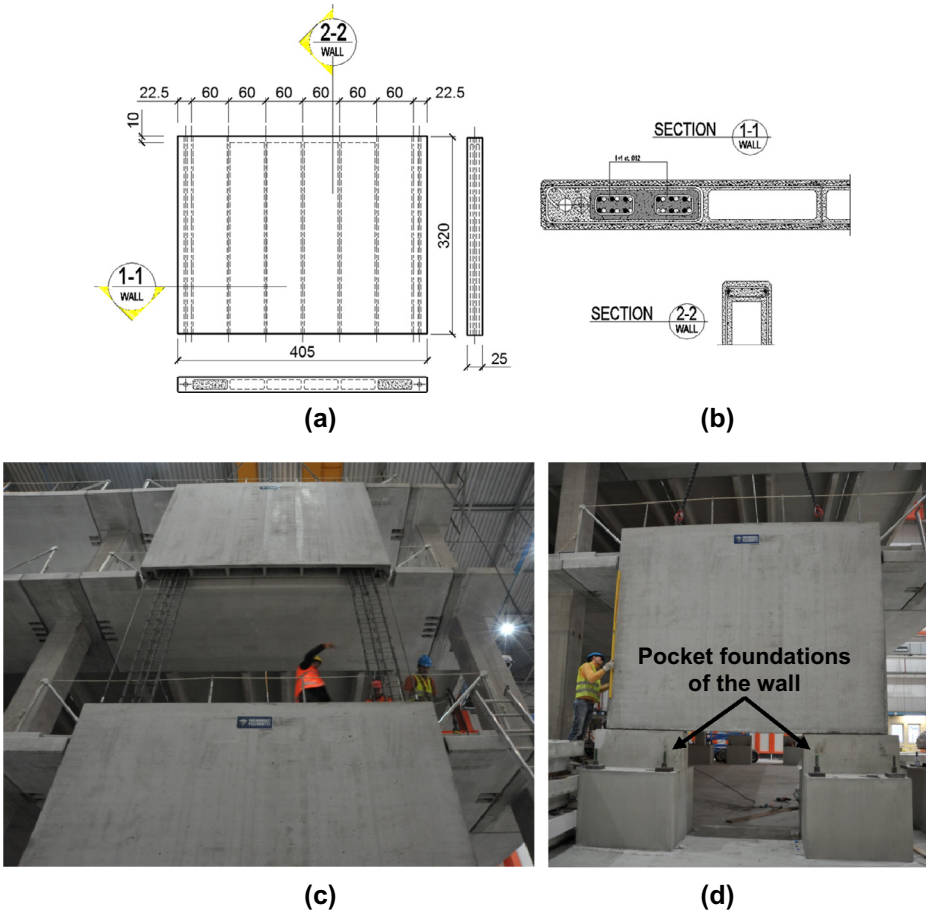

Fig. 4. (a) View of a hollow-core precast wall element. (b) Cross section of precast wall's end cores and flange. (c) Assembling phase of the precast wall elements. (d) Pocket foundations used for the precast wall elements (dimensions in cm).

high-resolution (2 μm) optical encoder displacement transducers, mounted on two reference unloaded frames (Fig. 6), and serving each one as feedback for the proportional-integral-derivative (PID) controller of one actuator.

Translational masses of 186,857 kg at the first floor, 168,404 kg at the second floor and 132,316 kg at the top floor, were numerically represented in the PsD test of prototype 1. The corresponding masses for the layouts without shear walls (prototypes 2, 3 and 4) were considered equal to 170,948 kg, 157,978 kg and 127,013 kg, for the first, second and third floor, respectively. The above simulated masses in the PsD tests are larger than the actual masses of the specimen in order to reproduce the effect of additional loads beyond self-weights. In the PsD test method it is not necessary to have the additional masses on the test structure physically

Table 1
Dimensions and percentages of steel reinforcement of all prefabricated bearing elements.

Precast and loading element	Concrete strength, f_c (MPa)	Type of the cross-section	Dimensions of the cross-section (m)	Amount of longitudinal reinforcement (mm^2)	Geometrical ratio of longitudinal reinforcement, ρ_s (%)
Column	64.5	Solid	0.5 × 0.5	2513	1.00
Beams of the 1st floor	64.5	Hollow-core	0.4 × 2.25	1810	0.35
Beams of the 2nd floor	64.5	Hollow-core	0.4 × 2.25	1609	0.32
Beams of the 3rd floor	64.5	Hollow-core	0.4 × 2.25	1473	0.29
Wall	64.5	Hollow-core	2.4 × 0.25	8952	1.30
Wall end	61	Solid	0.8 × 0.25	2767	1.38
Wall web	64.5	Hollow-core	2.45 × .25	3418	1.20

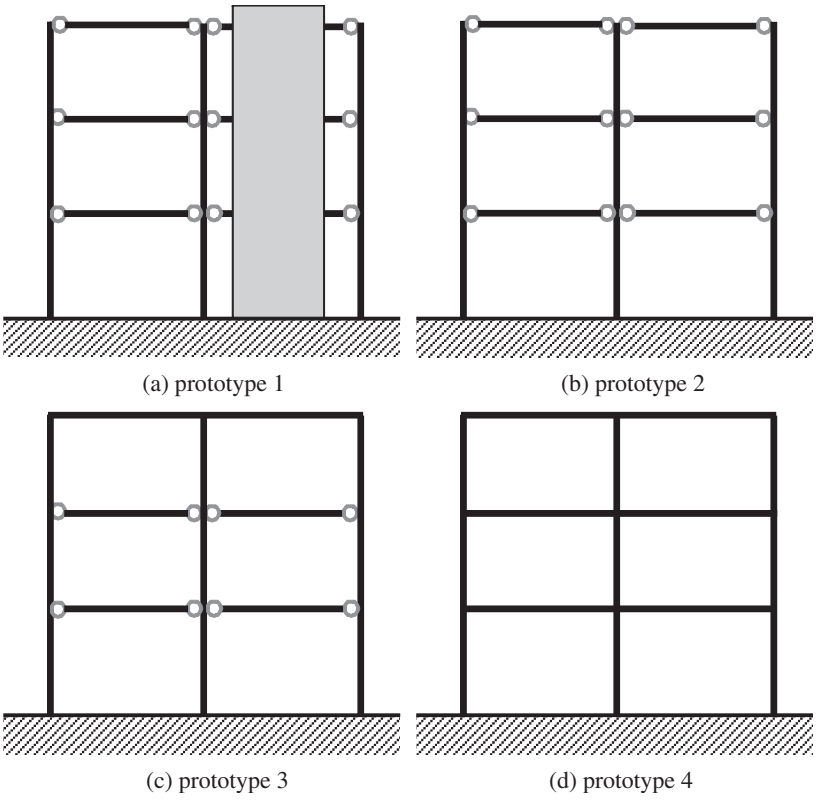

Fig. 5. Structural configuration of the prototype with: (a) Shear walls and hinged beam–column joints. (b) Hinged beam–column joints. (c) Hinged beam–column joints at the 1st and 2nd floor and emulative at the 3rd. (d) Emulative beam–column joints.

Table 2
Experimental parameters.

Specimen notation	Peak ground acceleration (g)	Existence of structural walls	Type of beam-to-column connection in the 1st and 2nd floor	Type of beam-to-column connection in the 3rd floor
Prot1_0.15g	0.15	Yes	Hinged	Hinged
Prot1_0.30g	0.30	Yes	Hinged	Hinged
Prot2_0.15g	0.15	No	Hinged	Hinged
Prot2_0.30g	0.30	No	Hinged	Hinged
Prot3_0.30g	0.30	No	Hinged	Emulative
Prot4_0.30g	0.30	No	Emulative	Emulative
Prot4_0.45g	0.45	No	Emulative	Emulative
Prot4_Cyc	Cyclic test	No	Emulative	Emulative

present, but only in the numerical model. Note that the possibility of using additional physical weights was rejected from the beginning of the project due to technical reasons. This restriction resulted into a slightly lower magnitude of the axial force in the columns. The average axial load ratios, $N/A_c f_c$, resulting for the columns of the ground floor are 0.029 or 0.027, for the prototype with or without shear walls, respectively. The corresponding axial load ratios, if the additional masses had been physically applied, would have been 0.034 and 0.032, respectively. No viscous damping term, $Cv(t)$, was included in the equation of motion of the PsD test algorithm Eq. (1), because in RC buildings the dissipation is hysteretic and is thus already reflected by the quasistatic relationship [15] of the (measured) restoring forces, $R(t)$, to the imposed displacement vector, $d(t)$.

An overview of the experimental set up adopted is shown in Fig. 6. The horizontal displacements were applied on the mid axis of the two transversal bays by two hydraulic actuators with a capacity of 1000 kN at the 2nd and 3rd floor levels, while at the 1st floor level (due to the availability of these devices in the laboratory), four actuators with capacity of 500 kN were used (two of which controlled in force). Steel beams were placed along the two actuator axes to connect all the floor elements and distribute the applied forces. An instrumentation network of 175 channels was used to measure:

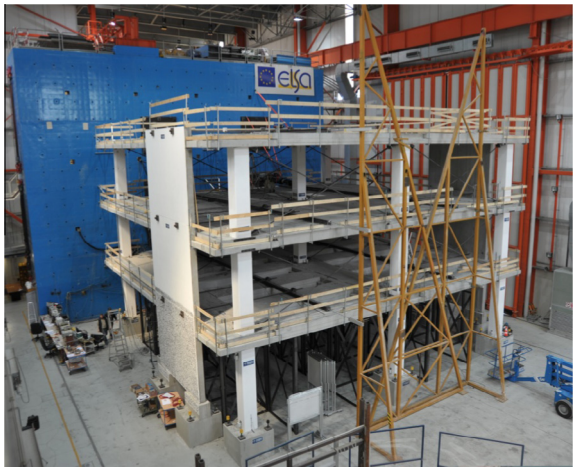

Fig. 6. General view of the experimental set-up.

1. The vertical deformation and curvature of the column sections at the base (bottom) of all columns of the ground storey.
2. Absolute rotations within the plane of testing of all ground storey columns, 300 mm above their bottom.
3. Absolute rotations within the plane of testing for the beams and columns in the vicinity of all beam–column joints of the central frame and one of the external frames.
4. The beam-to-column joint shear displacement measured in selected beam-to-column joints.
5. The decomposition of the wall lateral displacement at the first storey.

4.2. Input motion selection and test sequence

The reference input motion used in the PsD tests is a unidirectional 12 s-long time history, shown in Fig. 7a for a PGA of 1.0 g.

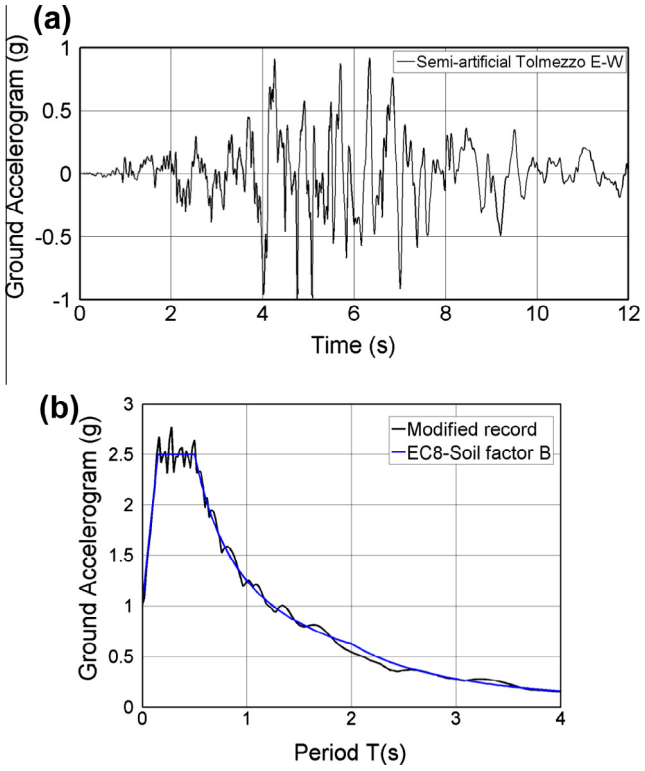

Fig. 7. (a) Input motion, scaled to PGA of 1 g. (b) Spectra of the modified EW component of the Tolmezzo record compared to EC8 spectrum.

The selected seismic action is represented by a real accelerogram (Tolmezzo 1976) modified to fit the Eurocode 8 (EC8) [16] response spectrum type B all over the considered frequency interval. Fig. 7b illustrates the spectra of the modified EW component of Tolmezzo recording and the EC8 specification. The accelerogram was scaled to the chosen peak ground accelerations of 0.15 g for the serviceability limit state, and 0.30 g for the no-collapse limit state. Two PsD tests at a PGAs of 0.15 g (Prot1_0.15g) and 0.30 g (Prot1_0.30g) were initially conducted on prototype 1, namely the dual frame-wall precast system. After the walls were disconnected from the structure, the same excitation sequence was repeated for prototype 2 (Prot2_0.15g and Prot2_0.30g) which had hinged beam–column connections in all joints. Prototype 3, which had emulative beam–column connections only at the top floor, was subjected only to the higher intensity earthquake of 0.30 g (Prot3_0.30g), whereas prototype 4 which had emulative connections in all beam–column joints, was tested at the PGAs of 0.30 g (Prot4_0.30g) and 0.45 g (Prot4_0.45g). A zero-acceleration signal was added after the end of the record, to allow for a free vibration of the test structures, giving total durations ranging between 15 s and 19 s for the applied record. To approach the ultimate capacity of the structure, a final "funeral" sequence of cyclic tests was performed, controlling the top displacement of the structure and constraining the floor forces to an inverted triangular distribution, which is consistent with the assumptions of most seismic codes including EC8.

5. Experimental results and discussion

Detailed results about the behaviour of the mechanical connections used between various precast elements are given in the companion paper by Bournas et al. In the next sections of this paper the global test results related to the overall pseudodynamic response of the four prototypes are presented in detail. A summary of the global response of all prototypes tested is given in Table 3. It includes: (a) The fundamental natural vibration period. (b) The maximum base shear in the two directions of loading. (c) The peak roof displacement. (d) The maximum interstorey drift of each floor. (e) The peak pseudo-acceleration at the roof.

5.1. Prototype 1 – structure with shear walls and hinged beam-to-column joints

Prototype 1 (Fig. 5a) was tested under two input motions scaled to a PGA of 0.15 g and 0.30 g. The time histories of floor displacements and restoring forces measured in these two PsD tests are shown in Fig. 8. As expected, this dual wall-frame precast system was stiff. A (experimental) fundamental natural vibration period of $T = 0.30$ s was observed for the 0.15 g PGA earthquake. The same fundamental period was obtained from a 0.03 g preliminary PsD test at the beginning of the test program. These period estimations, as for all the tests, were obtained from the measured response by means of identification of equivalent linear models [17]. Note that the theoretical fundamental period obtained from a three-dimensional model of the building using fully cracked walls ($I_{cr} = 0.33$ I_g, *where* I_g *is the stiffness for the gross section*) was slightly lower, namely $T = 0.28$ s. At the higher intensity earthquake, namely 0.30 g PGA, the response curves were characterized by lower frequencies (natural vibration period shifted to $T = 0.46$ s) due to the partial loss of tension stiffening in the vertical precast elements caused by the 0.15 g test. As can be observed in Fig. 8, the floor displacements and restoring forces are mostly in phase between them for both earthquake intensities, a fact which clearly indicates that the first vibration mode dominates the PsD response of this structural configuration.

Table 3
Summary of test results.

Specimen notation	Fundamental natural vibration period (s)	Maximum base shear (kN)		Peak roof displacement (mm)		Maximum interstory drift of each floor (%)						Peak roof acceleration (g)	
		Pull	Push	Pull	Push	Pull			Push			Pull	Push
						1st	2nd	3rd	1st	2nd	3rd		
Prot1_0.15g	0.30	1340	−1457	21.9	−16.8	0.12	0.24	0.31	0.15	0.19	0.21	0.44	−0.58
Prot1_0.30g	0.46	1780	−2146	48.2	−60.3	0.42	0.71	0.72	0.30	0.54	0.63	1.07	−0.91
Prot2_0.15g	1.09	500	−442	97.4	−86.6	0.58	1.12	1.28	0.57	0.99	1.08	0.31	−0.33
Prot2_0.30g	1.41	882	−895	208.2	−172.9	1.39	2.36	2.63	1.19	1.99	2.10	0.59	−0.64
Prot3_0.30g	1.08	889	−859	198.7	−148.4	1.74	2.54	1.77	1.37	1.91	1.23	0.50	−0.55
Prot4_0.30g	0.66	1715	−1454	132.5	−121.2	1.38	1.59	1.15	1.32	1.43	0.95	0.64	−0.88
Prot4_0.45g	1.25	1846	−1902	189.3	−206.5	1.96	2.37	1.77	2.46	2.37	1.45	0.98	−1.31
Cyclic test	–	2237	−2031	388.1	−415.6	6.01	4.63	1.96	5.93	5.05	2.01	–	–

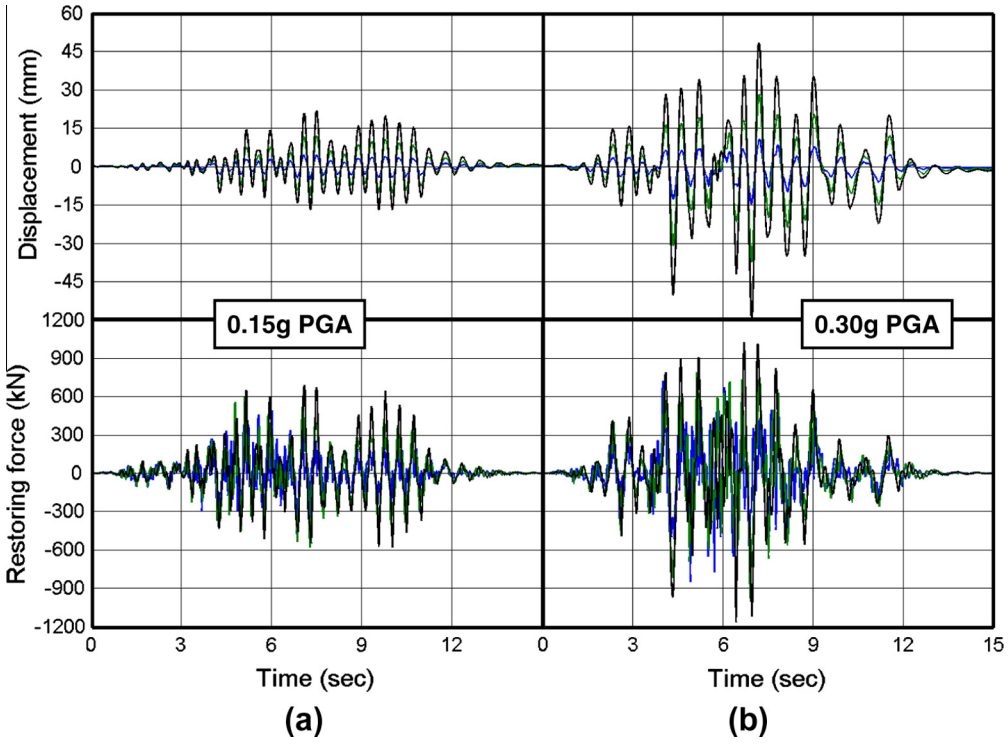

Fig. 8. Time histories of floor displacements and restoring forces of prototype 1 at PGAs of (a) 0.15 g and (b) 0.30 g.

The global base shear force versus roof (3rd floor) lateral displacement hysteretic response is plotted in Fig. 9 for the 0.15 g and 0.30 g tests. At the 0.15 g PsD test, corresponding to the serviceability limit state (SLS) earthquake, the response remained practically within the elastic range as it is illustrated in Fig. 9a. This PsD 0.15 g test deformed the building to a maximum roof displacement equal to 21.9 mm, while the maximum base shear force was 1457 kN. The maximum interstorey drift ratio was recorded at the third floor as equal to 0.31%. Fig. 9b plots the base shear versus roof displacement hysteretic curves for the 0.30 g test. At this higher intensity earthquake corresponding to the no-collapse design limit state, the response of the dual wall-frame system was characterized by some non-linear effects with noticeably wider force–displacement loops. The peak roof displacement and maximum base shear force measured in this test were 60.3 mm and 2146 kN, respectively. The maximum interstorey drift ratios recorded at the first, second and third floor remained at low levels, namely equal to 0.42%, 0.71% and 0.72%, respectively.

At the base of the ground level columns, moderate yielding occurred only in one of the loading directions for two columns, which reached a tensile strain (measured over the lower 300 mm of the column above the base and including the effect of bar pull-out from the base) of 0.29% and 0.31%, respectively, while the average tensile strain of all columns in both directions of loading was 0.22%. The average concrete compressive strain measured near the extreme compressive fibre, at the base of the 9 columns, remained in low levels in the 0.30 g test of prototype 1, namely 0.10%. The corresponding average tensile and compressive strains measured at the base of the two end sections (concealed columns) of the 2 walls, were 0.18% and 0.035%, respectively. These relatively low values of tensile and compressive strains, measured at the base of the walls, could be attributed to the fact that the contribution of flexural deformations comprises a small portion of their overall deformation, as explained in the next section.

The wall cracking pattern at the first floor after the 0.30 g PsD test is illustrated in Fig. 10a. Longitudinal and horizontal tensile

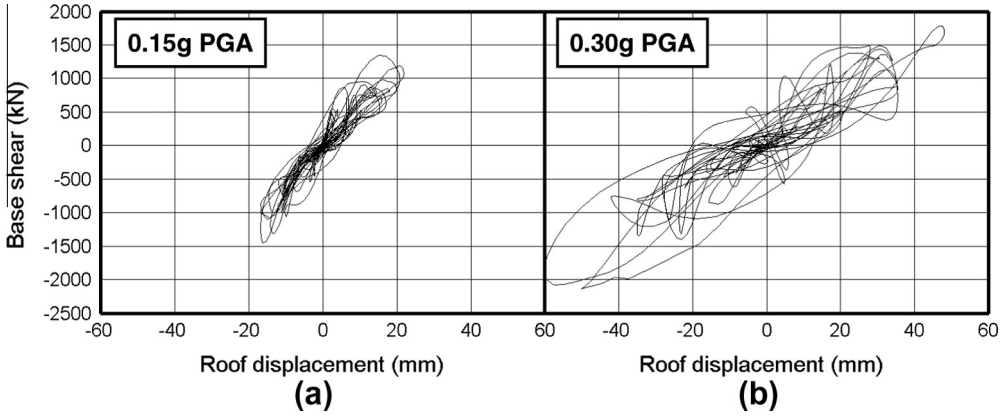

Fig. 9. Base shear versus roof displacement response of prototype 1 at PGAs of: (a) 0.15 g and (b) 0.30 g.

cracks were developed close to the wall end sections of maximum moment; these cracks were more evident over the lower 1 m from the wall base. Shear cracks were formed on the hollow web of the wall with an angle to the vertical direction approximately equal to 45° (Fig. 10a). The shear cracking initiated from the first seconds of the PsD test, whereas their number and length was increasing as the acceleration amplitudes was approaching the PGA of 0.30 g.

Despite the extensive cracking occurred on both shear walls, they did not reach significant level of damage their selves since the weak link in this layout was finally the wall-to-beam joint in each floor. In particular, the six beams connecting the two walls with the diaphragms failed in each floor due to diagonal compression (or shear) as shown in Fig. 10b. It should be pointed out here that the connection of the bracing walls with only two beams per floor was a sort of compromise arisen from the design of the testing programme, where (as mentioned above) the basic concept was to provide the capability of easily disconnecting the wall from the rest of the structure. To effectively transfer the shear forces from the floors into the walls, vertical shear connectors should be capacity designed and placed along the wall-to-floor interface. However, in spite of the fact that the walls did not reach their ultimate capacity, the main objectives of prototype 1, namely to reduce the flexibility of a multi-storey systems with hinged beam–column joints and to transfer high shear forces among slab-to slab and beam-to-column joints, were successfully met.

5.1.1. Decomposition of the wall lateral displacement

The overall wall drift is composed by various deformation mechanisms, namely deformations due to flexure, shear distortion, shear slip and fixed end rotation. In this section, an attempt is made to decompose the total wall displacement applied at the first floor into the above mentioned relative displacements by using the data recorded from the displacement transducers mounted on various cross sections of the walls. Fig. 11 illustrates the envelope of first floor drift (average of absolute values in both directions of loading) attributed to individual deformation mechanisms during the 0.30 g PsD test of prototype 1. In brief, based on this decomposition of the wall lateral drift at the first floor, it can be concluded that at the peak (0.45% drift) the shear distortion, shear slip, fixed-end rotation and the flexural contributions were equal to 25%, 17%, 41% and 17% of the total drift, respectively.

5.2. Prototype 2 – structure with hinged beam-to-column joints

Prototype 2 (Fig. 5b), which represents the most common connection system in the European construction practice with hinged beam-to-column connections, was tested under the 0.15 g and 0.30 g earthquakes. The time histories of floor displacements and restoring forces measured in these two PsD tests are shown in Fig. 12. The fundamental vibration period of this flexible structural system was $T = 1.10$ s for the 0.15 g PGA, whereas at the 0.30 g PGA, the response curves were characterized by lower frequencies (natural vibration period shifted to $T = 1.40$ s). The seismic response of prototype 2 was much influenced by the effect of higher modes. As can be observed in Fig. 12, the floor displacements and restoring forces are out of phase for both earthquake intensities at some moments. In addition, from the shape of the base shear force – top displacement curves, illustrated in Fig. 13, it is evident that the higher modes significantly influenced the values of storey forces, for both 0.15 g and 0.30 g earthquakes. Moreover, there seems to be no

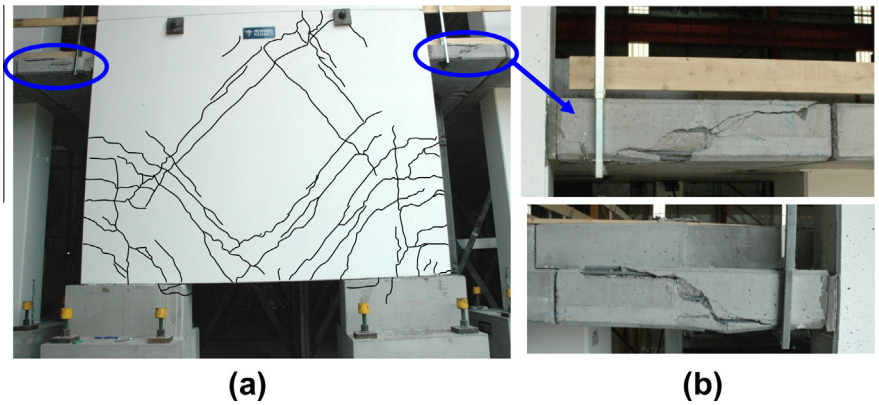

Fig. 10. (a) Cracking pattern of the wall at the 1st floor after the PGA 0.30 g. (b) Diagonal compression failure of the connection beams.

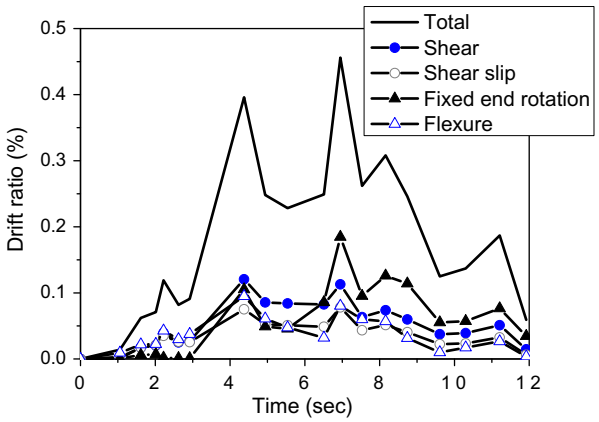

Fig. 11. Envelope of drift attributed to individual deformation mechanisms versus the total imposed drift for the first floor of the wall at PGA 0.30 g.

upper limit for the storey forces when the structure enters into the nonlinear regime, an effect which was anticipated in the preliminary nonlinear calculations [11]. This effect, which is a direct consequence of the large higher modes contribution, results into large force demands in the connections (companion paper, Bournas et al. [13]). To further evaluate the influence of the higher modes a modal decomposition is executed in the companion paper. It should be also pointed out here that, although the peaks of the input ground acceleration occurred during the first 7 s of the accelerogram (Fig. 7a), the corresponding peak floor displacements were recorded in its last 4 s, when the seismic excitation was considerably reduced. For this reason a zero-acceleration signal was added after the end of the record, to allow for a free vibration of the test structure, giving a total duration close to 19 s for the applied record.

At the 0.15 g PsD test, corresponding to the frequent (serviceability) seismic action, the overall response of prototype 2 remained practically within the elastic range as it is illustrated in Fig. 13a. However, the EC8 damage limitation requirement for buildings, which is simply expressed by an upper limit on the interstorey drift ratio, equal to 1% for the serviceability limit state was exceeded in the second and third floor. In particular, the maximum interstorey drifts were equal to 0.57%, 1.06%, and 1.18%, at the first, second and third storey, respectively. Thus, to meet the requirements imposed by EC8 a multi-storey hinged frame structure would require larger cross-sections of the columns. Fig. 13b plots the base shear versus roof displacement hysteretic curves for the 0.30 g test. At this higher intensity earthquake corresponding to the no-collapse design limit state, the response of this precast system with hinged beam-to-column joints was characterized by excessive deformability. The peak roof displacement and maximum base shear force measured in this test were 208 mm and 895 kN, respectively. Maximum interstorey drift ratios recorded at the first, second and third floor were 1.29%, 2.18% and 2.37%, respectively.

During the 0.30 g seismic excitation, yielding occurred at the base of the all ground level columns of prototype 2, which on average reached a tensile strain of 0.92%. The average concrete compressive strain measured near the extreme compressive fibre at the base of the 9 columns was 0.32%.

The behaviour of this structural configuration with hinged beam-to-column connections was in general satisfactory. Despite the limited stiffness of this structural configuration and the fact that the maximum interstorey drifts were above the limits imposed by EC8, prototype 2 did not suffer significant damage in its structural members during the 0.30 g PsD test. A visual inspection made at the end of the design level earthquake revealed only damages around the welding of the slab-to-slab connections of the first floor which are reported in the companion paper.

5.3. Prototype 3 – structure with emulative beam-to-column joints at the top

In the third structural configuration, the mechanical connection system embedded in the beam–column joints was activated to create moment-resisting connections only at the top floor and then prototype 3 (Fig. 5c) was subjected to the higher intensity earthquake of 0.30 g. The time histories of floor displacements and restoring forces measured in this PsD test are shown in Fig. 14. The fundamental vibration period of the structural system was reduced by 23% in comparison with its counterpart with hinged

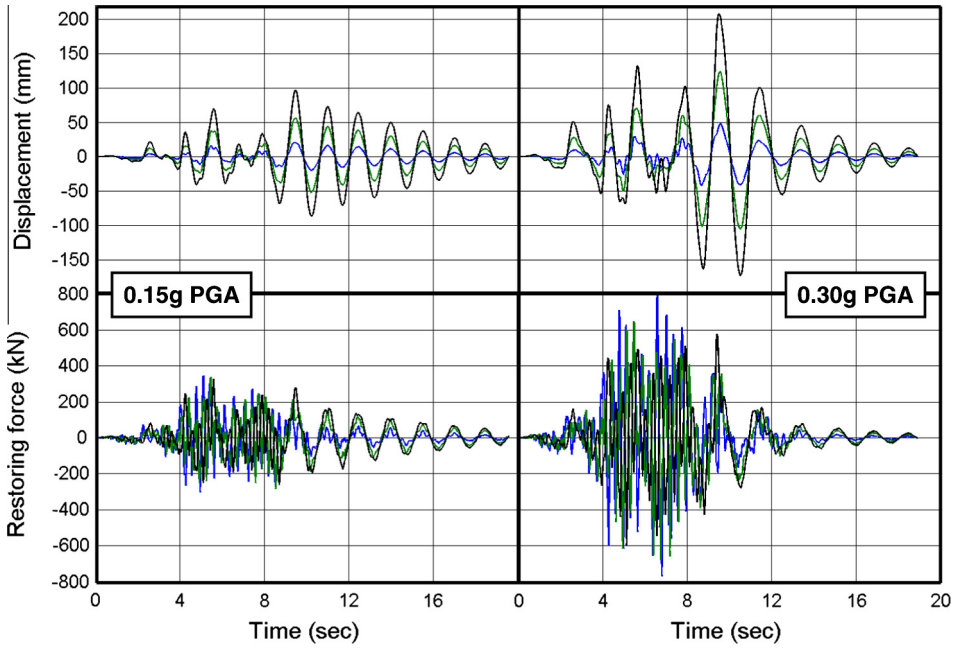

Fig. 12. Time histories of floor displacements and restoring forces of prototype 2 at PGAs of 0.15 g and 0.30 g.

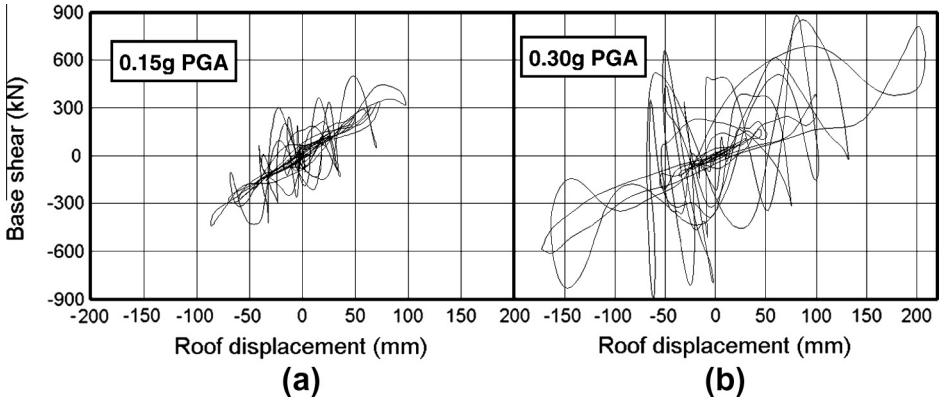

Fig. 13. Base shear versus roof displacement response of prototype 2 at PGAs of: (a) 0.15 g and (b) 0.30 g.

beam–column connections (T = 1.08 s, as opposed to T = 1.40 s in prototype 2). However, it turned out that the concept of emulative beam–column joints at the top floor only was not quite effective as a means of reducing interstorey drifts and the overall displacements of the structure. In fact, as illustrated in Fig. 14, the floor displacements and restoring forces are still out of phase for the design level earthquake a fact which, as in the case of prototype 2, corresponds to a seismic response considerably influenced by the effects of higher modes. As for prototype 2, the peak displacement response arose during the time interval 9.5–10.3 s, when the seismic input acceleration was marginal. Similarly to prototype 2, a zero-acceleration signal was added after the end of the record, to allow for a free vibration of the test structure, giving a total duration close to 19 s for the applied record.

Fig. 15 plots the base shear versus roof displacement hysteretic curves for the 0.30 g test. The peak roof displacement and maximum base shear force measured in this test were 199 mm and 889 kN, respectively. The maximum interstorey drifts were equal to 1.56%, 2.23%, and 1.50%, at the first, second and third storey, respectively. Comparing the above values to the corresponding maximum interstorey drifts marked in Prot2_0.30g, (namely 1.29%, 2.18% and 2.37%), it is evident that by constraining the beam–column joints of the top floor, the problem of large interstorey drifts was moved from the third to the second and first floors. Therefore, it appears that the damage limitation requirement for the serviceability limit state imposed by EC8, would not be met for the columns of lower stories by restraining only the top joints of a precast system with hinged beam–column connections.

Due to the restraining of the beam–column joints in the top floor, the seismic excitation of 0.30 g resulted in slightly higher stresses at the base of the ground floor columns. The average concrete tensile and compressive strain measured close to the extreme tension and compression fibre at the base of the 9 columns, were 1.22% and 0.39%, respectively. A visual inspection made at the end of the 0.30 g at prototype 3 did not reveal any new damages to the specimen.

5.4. Prototype 4 – structure with emulative beam-to-column joints

In the fourth and last layout, the mechanical connection system was activated in all beam–column joints with the aim of fully creating emulative moment-resisting frames. Prototype 4 (Fig. 5d) was tested under two input motions scaled to 0.30 g and 0.45 g. Fig. 16 illustrates the time histories of floor displacements and restoring forces measured during these two PsD tests. The natural vibration period of prototype 4 was 0.66 s, approximately half the period measured in its counterpart with hinged beam–column joints (Prot2_0.30g). This stiffer precast system led as a consequence to higher inertia forces and lower storey drifts. Moreover, its vibration for 0.30 g PGA was not affected by the higher modes to the same extent, as was the case in the prototypes with hinged beam-to-column joints. This can be clearly noticed in Fig. 16, where the restoring forces at the three floors are in phase with the applied horizontal floor displacements. At the maximum considered earthquake, namely 0.45 g PGA, though, the response curves were characterized by much lower frequencies (natural

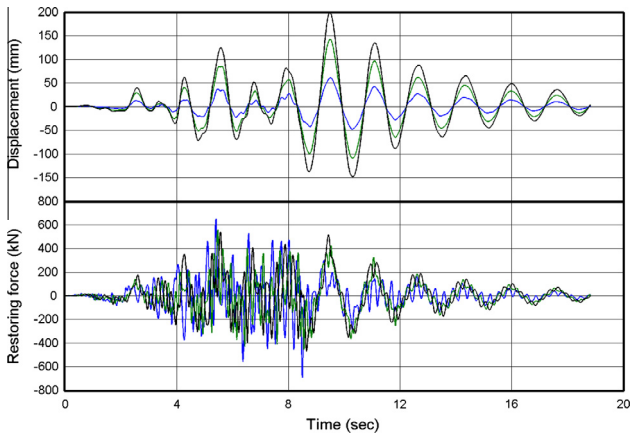

Fig. 14. Time histories of floor displacements and restoring forces of prototype 3 at PGA of 0.30 g.

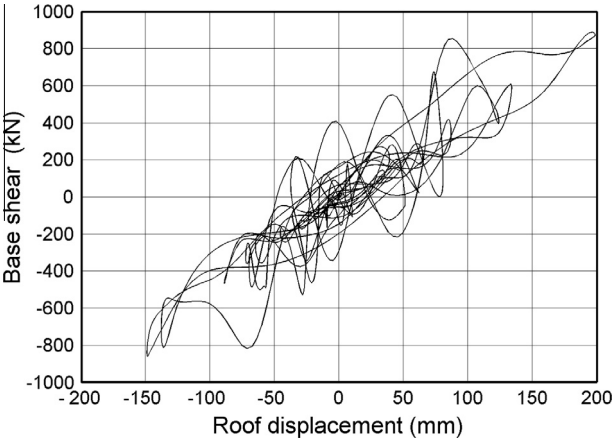

Fig. 15. Base shear versus roof displacement response of prototype 3 at PGA of 0.30 g.

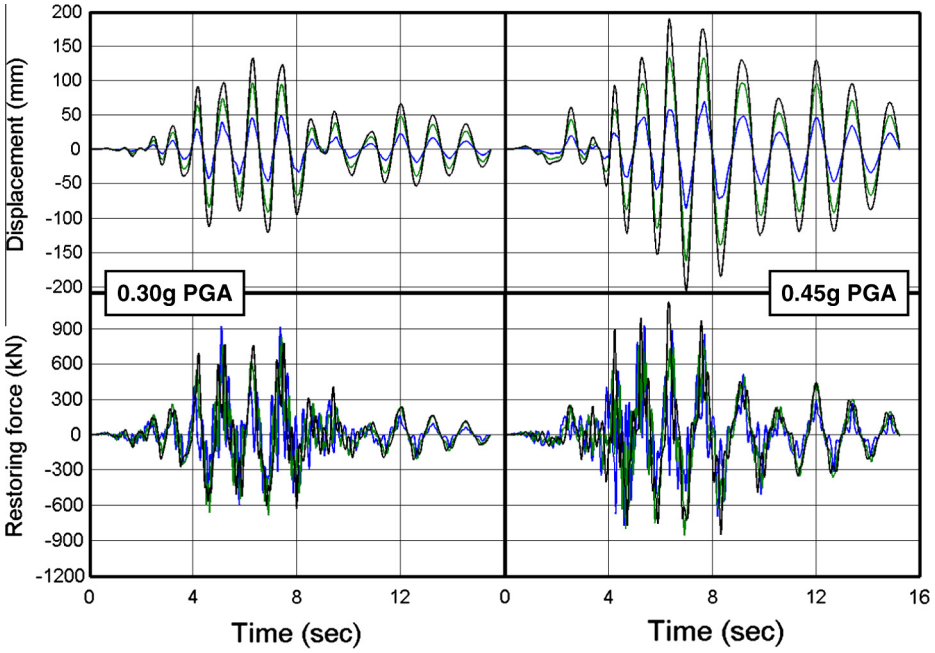

Fig. 16. Time histories of floor displacements and restoring forces of prototype 4 at PGAs of 0.30 g and 0.45 g.

vibration period shifted to $T = 1.25$ s) due to the crack opening of the beam–column joints, caused by the previous 0.30 g test.

Fig. 17 presents the base shear versus roof displacement loops of prototype 4 for both 0.30 g and 0.45 g earthquakes. In the ultimate limit state seismic excitation of 0.30 g, the response of prototype 4 underwent reduced non-linear effects (Fig. 17a). The 0.30 g PsD test deformed the building to a maximum roof displacement of 132.5 mm, while the maximum base shear force was 1454 kN. The maximum interstorey drifts were significantly lower than the corresponding ones in prototypes 2 and 3, namely they were equal to 1.35%, 1.51%, and 1.05%, at the first, second and third storey, respectively. The average concrete tensile and compressive strain measured close to the extreme tension and compression fibre at the base of the 9 columns, were 1.34% and 0.43%, respectively. A visual inspection made at the end of the 0.30 g at prototype 3 did not reveal any new damages to the specimen. Since prototype 4 survived the design level earthquake (0.30 g PGA) without significant damages, it was decided to proceed with the more intense seismic excitation of 0.45 g, which might be regarded as representative of the maximum considered earthquake (MCE).

The peak roof displacement and maximum base shear force measured in this test were 206.5 mm and 1902 kN, respectively. Under the 0.45 g excitation, the maximum interstorey drifts were increased to 2.21%, 2.37%, and 1.61%, at the first, second and third storey, respectively. A visual inspection of the structure after the 0.45 g PsD test revealed dense flexural cracking at the base of the ground floor columns, but without considerable damage. The average concrete tensile and compressive strain measured (near the extreme tension compression fibre) at the base of the 9 columns were 2.61% and 0.60%, respectively. Additionally, the flexural cracking detected at the bottom of beams, in the vicinity of the beam–column joints of the first and second floor, indicated evidence of yielding at those cross-sections. At the end of 0.45 g test, the width of the permanent cracks measured at the base of ground floor columns and at the bottom of beams in the first and second floor, was approximately 0.2 mm and 0.1 mm, respectively. No clear identification of the plastic mechanism was possible at this level of deformation.

In summary, the PsD test results show that the proposed connection system is quite effective as a means of implementing dry precast (quasi) emulative moment-resisting frames especially when all beam–column joints are made rigid.

5.5. Final cyclic test

Peak ground accelerations of 0.30 g or 0.45 g could be assumed to be the intensities for the no-collapse limit state for a zone with high seismicity, however, the seismic tests did not lead prototype 4

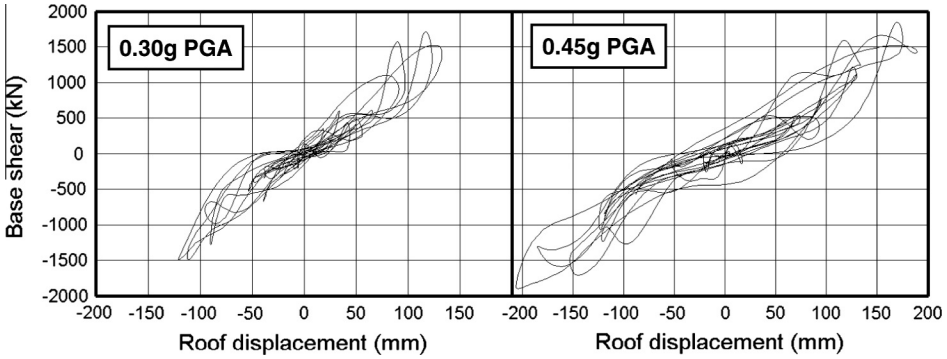

Fig. 17. Base shear versus roof displacement response of prototype 4 at PGAs of: 0.30 g and 0.45 g.

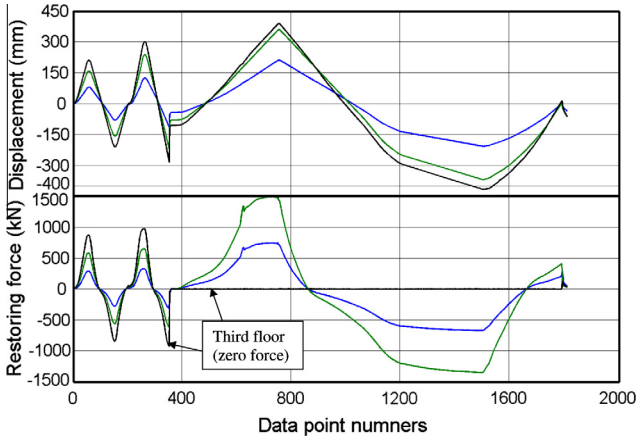

Fig. 18. Time histories of floor displacements and restoring forces of prototype 4 during the cyclic test.

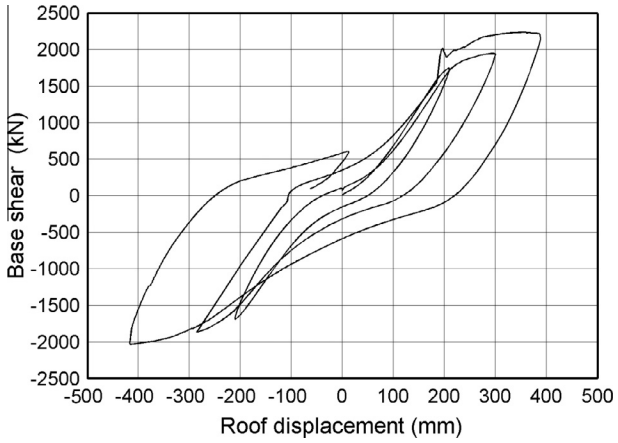

Fig. 19. Base shear versus roof displacement response of prototype 4 during the cyclic test.

to heavy damage. To approach the ultimate capacity of the structure, a final "funeral" sequence of cyclic tests has been performed, controlling the top displacement of the structure and constraining the floor forces to an inverted triangular distribution. The starting displacement amplitude was selected to approximately coincide with the maximum displacement recorded during the PsD tests, while the successive cycle(s) progressively increasing by 90 mm corresponded roughly to 1% interstorey drift increases. Two cycles were repeated at increasing amplitudes of ±210 mm and ±300 mm. During the reverse cycle of the larger amplitude (300 mm), the fastenings of one of the actuator force distribution beams were detached at the third floor. For this reason the final loading cycle of the test was performed by applying the actions only at the first and second floors and controlling the displacement at the second floor at ±360 mm amplitude. The fact that the actuators of the third floor were disconnected during the last cycle, therefore applying zero force, did not drastically affect the building's maximum base shear force, nor its "collapse" mechanism, since the damage concentration and interstorey drifts measured already during the two cycles (amplitudes of ±210 mm and ±300 mm), were in the 1st and 2nd floor substantially higher than in the 3rd one.

Fig. 18 illustrates the time histories of floor displacements and restoring forces measured during the cyclic test in prototype 4. The maximum interstorey drifts were considerably high, namely

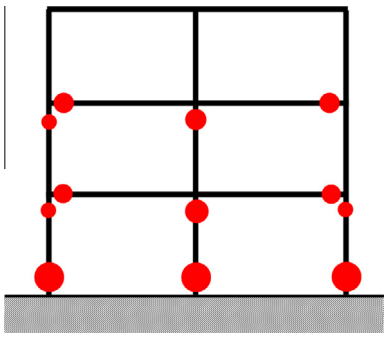

Fig. 20. Typical damage pattern and plastic hinging formation after the cyclic test.

equal to 5.97%, 4.84%, and 1.99%, at the first, second and third storey, respectively. Fig. 19 presents the base shear versus roof displacement hysteretic curves recorded for the cyclic test. The peak roof displacement and maximum base shear force measured in the cyclic test were 415.6 mm (4.2% global drift) and 2237 kN, respectively. During the cyclic test, the response of prototype 4 underwent extensive damages and approached the non-collapse limit state with very wide force-drift cycles. Nevertheless, even under the very high horizontal displacements that prototype 4 was subjected to, its peak recorded strength was not considerably reduced in any of the loading directions and thus the building's failure as it is conventionally defined (20% drop in peak strength) was not reached. The cyclic test was terminated when the stroke of the actuators in the first floor (±250 mm) was about to be exhausted.

The damage pattern and the distribution of plastic hinge formation detected in each frame of prototype 4 after the cyclic test is summarized in Fig. 20, where the size of the circles approximately indicates the level of damage identified and also estimated on the basis of the permanent crack width. The major part of inelasticity and damage was concentrated at the base of all ground floor columns, namely at the cross-sections of maximum moment. There, the concrete cover and part of the core over the lower 300 mm of the columns disintegrated and bar buckling initiated after the concrete cover spalled off, as shown in Fig. 21a. The average maximum concrete tensile and compressive strains(for the 9 columns) at those sections were excessive, (7.61% and 3.24%, respectively). The ground floor columns attained a drift ratio of about 6% (Fig. 21b), while their mean curvature ductility factor μ_ϕ was rather high, in the order of 22.

The plastic hinge formation was then diffused at the joints of the first and second storey. It appears that at the first floor level, the capacity design requirements (plastic hinges to appear in beam rather than column ends) were not met in all beam–column joints. In particular, for the external joints, where the column was framing into only one beam, it seems that the plastic hinge was formed in the beams (primarily) but also in the columns. The cracking at these joints started in the vicinity of the mechanical connections, possibly due to debonding forces, and propagated to the adjacent beam and column, as illustrated in Fig. 22a. On the other hand, at the 3 central joints, where two beams were connected to each column, the plastic hinge was clearly developed in the columns and the beams remained essentially intact (Fig. 22b). The damage pattern was identical in the joints of the second floor, even though the damage accumulation was clearly inferior there.

6. Conclusions

A full-scale three-storey precast building was subjected to a series of PsD tests in the European Laboratory for Structural Assess-

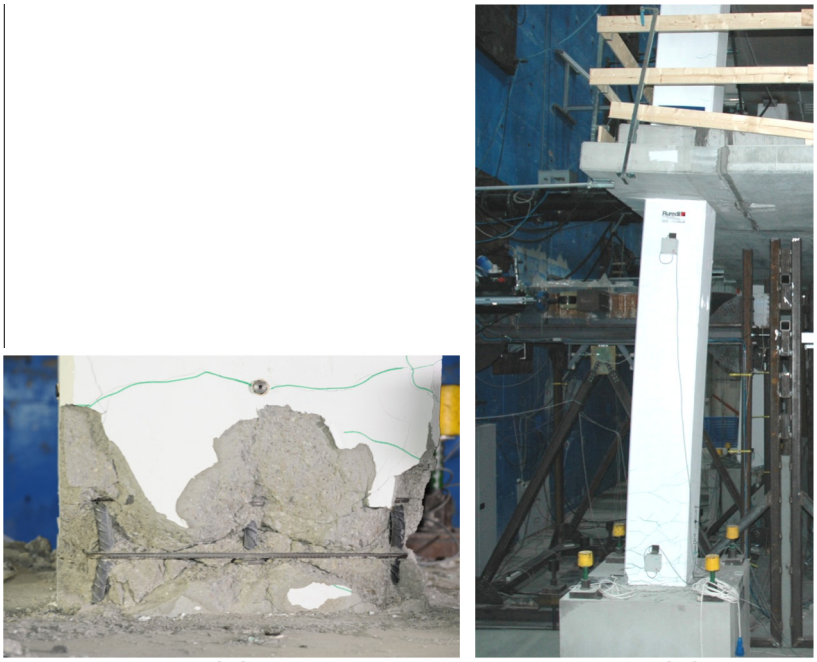

Fig. 21. Final damage state: (a) Disintegration of concrete and bar buckling. (b) View of the first floor's columns (approximately) maximum horizontal displacement during the cyclic test.

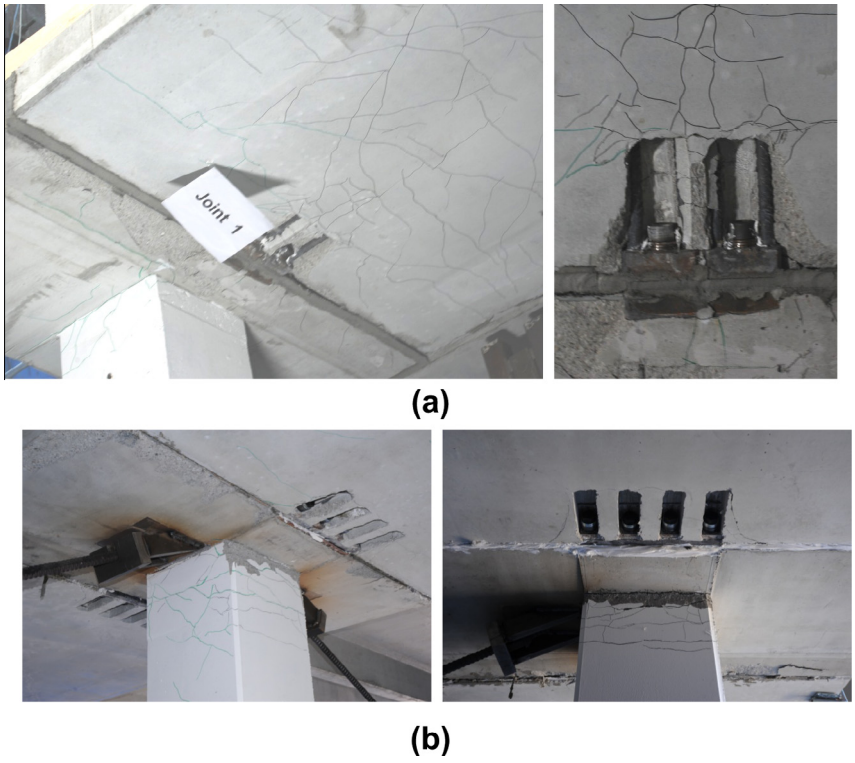

Fig. 22. Final damage state: (a) Cracking in the vicinity of an external first floor's (emulative) beam–column joint. (b) Plastic hinging at the top of the first floors' columns in a central beam–column joint.

ment. The mock-up was constructed in such a way that four different structural configurations were investigated experimentally. Therefore, the behaviour of various parameters like the types of mechanical connections (traditional as well as innovative) and the presence or absence of shear walls along with the framed structure were assessed.

The presence of two stiff precast wall units in prototype 1 was quite effective in limiting the maximum interstorey drift ratios for

both the serviceability and ultimate limit states. In such a dual frame-wall system the first vibration mode dominated the PsD response for both earthquake intensities. However the proper connection of stiff RC walls or cladding elements to precast diaphragms still remains a challenging task.

The seismic response of prototype 2 was highly influenced by the effects of higher modes. There seemed to be no upper limit for the storey forces when the structure entered into the nonlinear regime. This effect, which is a direct consequence of the large higher modes contribution, results into large force demands in the connections. The 1% drift limitation imposed by EC8 for the SLS was exceeded and, at the higher intensity earthquake, corresponding to ULS, the response of this precast system with hinged beam-to-column joints was characterized by excessive deformability. However, despite the limited stiffness of this structural configuration and the fact that the maximum interstorey drifts were above the limits imposed by EC8, prototype 2 did not suffer significant damage in its structural members during the 0.30 g PsD test. A visual inspection made at the end of the design level earthquake revealed only some very slight damages.

After the seismic test results of prototype 3, it turned out that the concept of emulative beam–column joints at the top floor only was not much effective as a means of reducing interstorey drifts and the overall displacements of the structure, as well as controlling the effect of higher modes on the structure's seismic response.

Finally, when activated at all the floors, the proposed connection system is quite effective as a means of implementing dry precast (quasi) emulative moment-resisting frames. This was the case in prototype 4, where lower maximum interstorey drifts were recorded and the first vibration mode dominated the PsD response. In the design level test (0.30 g), prototype 4 underwent little non-linear effects and thus it was subjected to a PGA of 0.45 g. In this MCE the structure revealed dense flexural cracking at the base of the ground floor columns, but again without considerable damage. In the final cyclic test, prototype 4 underwent extensive damages and approached the non-collapse limit state with very wide force-drift cycles. The major part of inelasticity and damage was concentrated at the base of all ground floor columns which attained a drift ratio of about 6%.

Acknowledgements

The research has been addressed within the SAFECAST project (Grant agreement no. 218417-2), a three-year project (2009–2012) financed by the European Commission within the Seventh Framework Programme. The authors wish to thank the whole ELSA technical team for their assistance in the experimental programme.

References

[1] Saisi A, Toniolo G. Precast r.c. columns under cyclic loading: an experimental program oriented to EC8. Studi e Ricerche, vol. 19. School for Concrete Structures "F.lli Pesenti", Politecnico di Milano; 1998. p. 373–414.
[2] Ferrara L, Colombo A, Negro P, Toniolo G. Precast vs. cast-in-situ reinforced concrete industrial buildings under earthquake loading: an assessment via pseudodynamic tests. In: Proc of the 13th WCEE, 2004.
[3] Negro P, Mola E, Ferrara L, Zhao B, Magonette G, Molina J. PRECAST STRUCTURES EC8: seismic behaviour of precast concrete structures with respect to EC8-Contract N. G6RD-CT – 2002-00857. Final report of the experimental activity of the Italo-Slovenian Group; 2007. 190p.
[4] Moguruma H, Nishiyama M, Watanabe F. Lessons learned from the Kobe earthquake – a Japanese perspective. PCI J 1995;40(4):28–42.
[5] EERI. Kocaeli, Turkey, Earthquake of August 17, 1999 Reconnaissance report, earthquake spectra, vol. 16 (Suppl.); 2000.
[6] Saatcioglu M, Mitchell D, Tinawi R, Gardner NJ, Gillies AG, Ghobarah A, Anderson DL, Lau D. The August 17, 1999 Kocaeli (Turkey) earthquake-damage to structures. Can J Civ Eng 2001;28(8):715–73.
[7] Tzenov LL, Sotirov, Boncheva P. Study of some damaged industrial buildings due to Vrancea earthquake. In: Proc of 6th ECEE, vol. 6. Dubrovnik; 1978. p. 59–65.
[8] Fajfar P, Duhovnik J, Reflak J, Fischinger M, Breška Z. The behaviour of buildings and other structures during the earthquakes of 1979 in Montenegro, vol. 19A. University of Ljubljana, Department of Civil Engineering: Institute of Structural and Earthquake Engineering. IKPIR Publication; 1981. 183pp.
[9] EERI. Northridge Earthquake January 17, 1994. Preliminary reconnaissance report. Earthquake Engineering Research Institute; 1994. 104p.
[10] EERI. Armenia Earthquake Reconnaissance Report, Earthquake spectra. Earthquake Engineering Research Institute; 1989. 175p.
[11] Olgiati M, Negro P, Colombo A. SAFECAST project: definition and analysis of the three-storey precast buildings. In: Proc of the 14th ECEE; 2010.
[12] Fischinger M, Kramar M, Isaković T. The selection of the accelerogram to be used in the experimental program-selection of the record for 3-storey full-scale structure to be tested at ELSA, JRC. SAFECAST – UL Report No. 4a; 2010. 66p.
[13] Bournas DA, Negro P, Molina FJ. Pseudodynamic tests on a full-scale 3-storey precast concrete building: behavior of the mechanical connections and floor diaphragms. Elsevier Eng Struct J 2012. 58C.
[14] Pegon P, Molina FJ, Magonette G. Continuous pseudo-dynamic testing at ELSA. In: Saouma VE, Sivaselvan MV, editors. Hybrid simulation; theory, implementation and applications. Taylor & Francis/Balkema Publishers; 2008. p. 79–88.
[15] Molina FJ, Magonette G, Pegon P, Zapico B. Monitoring damping in pseudo-dynamic tests. J Earthq Eng 2011;15(6):877–900.
[16] CEN. European Standard EN 1998-3: Eurocode 8: design of structures for earthquake resistance – Part 3: Assessment and retrofitting of buildings, European committee for standardization, Brussels, 2005.
[17] Molina FJ. Spatial and filter models. MATLAB functions freely available at MATLAB central file exchange. Natick, Massachusetts (USA): The MathWorks, Inc.; 2011. <http://www.mathworks.com/matlabcentral/fileexchange/32634> [22.08.11].